
This copy is for your personal, non-commercial use only.

If you wish to distribute this article to others, you can order high-quality copies for your colleagues, clients, or customers by [clicking here](#).

Permission to republish or repurpose articles or portions of articles can be obtained by following the guidelines [here](#).

The following resources related to this article are available online at www.sciencemag.org (this information is current as of June 6, 2011):

Updated information and services, including high-resolution figures, can be found in the online version of this article at:

<http://www.sciencemag.org/content/332/6034/1186.full.html>

Supporting Online Material can be found at:

<http://www.sciencemag.org/content/suppl/2011/05/11/science.1201425.DC1.html>

A list of selected additional articles on the Science Web sites **related to this article** can be found at:

<http://www.sciencemag.org/content/332/6034/1186.full.html#related>

This article has been **cited by** 1 articles hosted by HighWire Press; see:

<http://www.sciencemag.org/content/332/6034/1186.full.html#related-urls>

This article appears in the following **subject collections**:

Planetary Science

http://www.sciencemag.org/cgi/collection/planet_sci

augments the radial pressure force to the point that magnetic tension in the geostationary magnetosphere can no longer contain the fluid, not even in the dawn-dusk meridian. In this sense, the convection cycle of a sawtooth substorm resembles the Vasyliunas cycle (41) at Jupiter, wherein corotating, mass-loaded flux tubes pinch off to form plasmoids in the pre-midnight sector, then cyclically refill after rotating around the magnetosphere again. The Vasyliunas cycle at Jupiter is periodic in space; its analog at Earth is periodic in time. Jupiter's periodic cycle is powered by planetary rotation; in contrast, Earth's cycle is powered by the SW-M dynamo and its propensity to produce ionospheric outflows.

Although we have shown that ionospheric outflow in MHD simulations can produce the sawtooth convection mode, we do not know if it is the only (or the most important) mechanism.

References and Notes

1. R. D. Belian, T. E. Cayton, *Proc. Res. Inst. Atmos. Nagoya Univ.* **36**, 127 (1989).
2. J. E. Borovsky, R. J. Nemzek, R. D. Belian, *J. Geophys. Res.* **98**, 3807 (1993).
3. C. Huang *et al.*, *J. Geophys. Res.* **108**, 1255 (2003).
4. K. Kitamura, H. Kawano, S. Ohtani, A. Yoshikawa, K. Yumoto, *J. Geophys. Res.* **110**, A07208 (2005).
5. X. Cai, M. G. Henderson, C. R. Clauer, *Ann. Geophys.* **24**, 3481 (2006).
6. M. G. Henderson *et al.*, *J. Geophys. Res.* **111**, A01590 (2006).
7. O. Troshichev, A. Janzhura, *J. Atmos. Sol. Terr. Phys.* **71**, 1340 (2009).
8. C. Huang, *Geophys. Res. Lett.* **29**, 2189 (2002).
9. X. Cai, C. R. Clauer, *J. Geophys. Res.* **114**, A06201 (2009).
10. I. Mann, A. Wright, K. Mills, V. Nakariakov, *J. Geophys. Res.* **104**, 333 (1999).
11. V. A. Sergeev, *Phys. Sol. Terr. Potsdam* **5**, 39 (1977).
12. T. Pytte, R. L. McPherron, E. W. Hones Jr., H. I. West Jr., *J. Geophys. Res.* **83**, 663 (1978).
13. V. A. Sergeev, R. J. Pellinen, T. I. Pulkkinen, *Space Sci. Rev.* **75**, 551 (1996).
14. R. L. McPherron, T. P. O'Brien, S. Thompson, in *Multiscale Coupling of Sun-Earth Processes*, A. T. Y. Lui, Y. Kamide, G. Consolini, Eds. (Elsevier, Amsterdam, 2005), pp. 113–124.
15. R. M. Winglee, D. Chua, M. Brittner, G. K. Parks, G. Lu, *J. Geophys. Res.* **107**, 1237 (2002).
16. A. Gloer, G. Toth, T. Gombosi, D. Welling, *J. Geophys. Res.* **114**, A05216 (2009).
17. M. Wiltberger, T. Pulkkinen, J. Lyon, C. Goodrich, *J. Geophys. Res.* **105**, 27649 (2000).
18. J. Raeder, D. Larson, W. Li, E. L. Kepko, T. Fuller-Rowell, *Space Sci. Rev.* **141**, 535 (2008).
19. C. C. Goodrich, T. I. Pulkkinen, J. G. Lyon, V. G. Merkin, *J. Geophys. Res.* **112**, A08201 (2007).
20. T. I. Pulkkinen, C. C. Goodrich, J. G. Lyon, *Geophys. Res. Lett.* **34**, L21101 (2007).
21. B. Lavraud, J. E. Borovsky, *J. Geophys. Res.* **113**, A00B08 (2008).
22. M. M. Kuznetsova *et al.*, *J. Geophys. Res.* **112**, A10210 (2007).
23. E. Shelley, R. Johnson, R. Sharp, *J. Geophys. Res.* **77**, 6104 (1972).
24. M. Nosé *et al.*, *J. Geophys. Res.* **110**, A09524 (2005).
25. B. Thelin, B. Aparicio, R. Lundin, *J. Geophys. Res.* **95**, 5931 (1990).
26. Y.-K. Tung *et al.*, *J. Geophys. Res.* **106**, 3603 (2001).
27. A. Keiling, J. R. Wygant, C. A. Cattell, F. S. Mozer, C. T. Russell, *Science* **299**, 383 (2003).
28. C. C. Chaston, C. W. Carlson, J. P. McFadden, R. E. Ergun, R. J. Strangeway, *Geophys. Res. Lett.* **34**, L07101 (2007).
29. C. C. Chaston *et al.*, *J. Geophys. Res.* **109**, A04205 (2004).
30. C. E. Seyler, K. Liu, *J. Geophys. Res.* **112**, A09302 (2007).
31. P. Norqvist, M. André, M. Tyrlund, *J. Geophys. Res.* **103**, 23459 (1998).
32. J. Lyon, J. Fedder, C. Mobarry, *J. Atmos. Sol. Terr. Phys.* **66**, 1333 (2004).
33. O. Brambles *et al.*, *J. Geophys. Res.* **115**, A00J04 (2010).
34. Variations in outflow flux with electromagnetic power input may be due to seasonal or solar cycle influences on the source population or to variations in preconditioning of the M-I system before the initiation of a sawtooth event. In addition, the simulation model may not accurately replicate the power typically observed in the Alfvénic band (see SOM).
35. C. M. Cully, E. F. Donovan, A. W. Yau, G. G. Arkos, *J. Geophys. Res.* **108**, 1093 (2003).
36. V. M. Vasyliunas, J. R. Kan, G. L. Siscoe, S.-I. Akasofu, *Planet. Space Sci.* **30**, 359 (1982).
37. A. D. DeJong, A. J. Ridley, X. Cai, C. R. Clauer, *J. Geophys. Res.* **114**, A08215 (2009).
38. The reconnection in the LFM code is predominantly averaging error; opposing magnetic flux enters a single cell and is averaged (annihilated) out of existence (32). The rate of reconnection is sensitive to the conditions external to the actual reconnection region. In cases where the external flow toward the reconnection site is zero, the reconnection is effectively also zero. When reconnection is driven (that is, forced by convergent flow), the rate can be quite high. The maximum rate is constrained by a Petschek-like inflow condition to be a fraction (~0.1) of the Alfvén speed in the inflow.
39. For zero dipole tilt angle in these simulations, MLT is similar to geographic local time, where 1200 MLT always directly faces the sun.
40. J. W. Dungey, *Phys. Rev. Lett.* **6**, 47 (1961).
41. V. M. Vasyliunas, in *Physics of the Jovian Magnetosphere*, A. J. Dessler, Ed. (Cambridge Univ. Press, New York, 1983), pp. 395–453.
42. Y. I. Feldstein, G. V. Starkov, *Planet. Space Sci.* **18**, 501 (1970).
43. M. Wiltberger, R. S. Weigel, W. Lotko, J. A. Fedder, *J. Geophys. Res.* **114**, A01204 (2009).
44. P. Banks, T. Holzer, *J. Geophys. Res.* **73**, 6846 (1968).
45. W. Baumjohann, R. A. Treumann, *Basic Space Plasma Physics* (Imperial College Press, London, 1996), chap. 2.
46. A.W. Yau, M. André, *Space. Sci. Rev.* **80**, 1 (1997).
47. B. Hultqvist, M. Oieroset, G. Paschmann, R. Treumann, Eds., *Magnetospheric Plasma Sources and Losses* (Springer, New York, 1999).
48. R. J. Strangeway, R. E. Ergun, Y. Su, C. W. Carlson, R. C. Elphic, *J. Geophys. Res.* **110**, A03221 (2005).
49. G. Paschmann, S. Haaland, R. Treumann, Eds., *Auroral Plasma Physics* (Space Sciences Series of ISSI, Kluwer Academic, Dordrecht, Netherlands, 2003), pp. 70–74.
50. M. Bouhram *et al.*, *Ann. Geophys.* **22**, 1787 (2004).
51. W. Lotko, *J. Atmos. Sol. Terr. Phys.* **66**, 1443 (2004).

Acknowledgments: This research was supported by the NASA Sun-Earth Connection Theory Program (grant NNX08AI36G), the NASA Living With a Star Targeted Research and Technology Program (grants NNX07AQ16G and NNX07AT15G), and the Center for Integrated Space Weather Modeling funded by the NSF Science and Technology Centers program under cooperative agreement ATM-0120950. Computing resources for the research were provided by the National Center for Atmospheric Research under Computational Information Systems Laboratory Project 36761008. The National Center for Atmospheric Research is supported by NSF. Simulation data are available from O. Brambles. FAST satellite data are available online at <http://sprg.ssl.berkeley.edu/fast/>.

Supporting Online Material

www.sciencemag.org/cgi/content/full/332/6034/1183/DC1
SOM Text
Figs. S1 and S2
References (43–51)

14 January 2011; accepted 27 April 2011
10.1126/science.1202869

Evidence of a Global Magma Ocean in Io's Interior

Krishan K. Khurana,^{1*} Xianzhe Jia,² Margaret G. Kivelson,^{1,2} Francis Nimmo,³ Gerald Schubert,¹ Christopher T. Russell¹

Extensive volcanism and high-temperature lavas hint at a global magma reservoir in Io, but no direct evidence has been available. We exploited Jupiter's rotating magnetic field as a sounding signal and show that the magnetometer data collected by the Galileo spacecraft near Io provide evidence of electromagnetic induction from a global conducting layer. We demonstrate that a completely solid mantle provides insufficient response to explain the magnetometer observations, but a global subsurface magma layer with a thickness of over 50 kilometers and a rock melt fraction of 20% or more is fully consistent with the observations. We also place a stronger upper limit of about 110 nanoteslas (surface equatorial field) on the dynamo dipolar field generated inside Io.

Io, the most volcanic planetary body in the solar system, is known for its prodigious thermal output [$>2 \text{ W/m}^2$, roughly 30 times Earth's averaged output, (1, 2)]. Gravity studies suggest (3) that Io's differentiation has resulted in a metallic iron core with a radius of 650 to 950 km,

surrounded by a mantle believed to be peridotitic (4) with a density of 3250 to 3700 kg m^{-3} and forsterite (Mg_2SiO_4) likely the most abundant mineral (5). Extensive volcanism has probably created a lower-density, cold, rigid outer crust (6). Surface lava temperatures hint at an upper-mantle

temperature of 1250° to 1450°C, suggesting that beneath the crust there lies a fully or partially molten layer [the asthenosphere (7, 8)], but its existence and state are matters of considerable debate (9–12). Here we interpret magnetic field measurements made near Io as strengthening the evidence for such a layer.

Induction caused by Jupiter's rotating magnetic field was previously used to identify electrically conducting subsurface oceans in the icy satellites Europa, Ganymede, and Callisto (13–15). At Io, too, the inductive response can be used to infer the properties of its interior, because the conductivities of subsurface layers depend on the temperatures and the melt states of their constituent rocks (16–19). The conductivities of dry solid ultramafic rocks increase from 10^{-9} S/m at room temperature (20) to $\sim 10^{-3}$ S/m at 1200°C and $\sim 10^{-2}$ S/m at 1400°C at pressures prevailing in Io's upper mantle (17, 18). Ultramafic rock melts have conductivities in the range of 1 to 5 S/m at 1200° to 1400°C, and partially molten rocks have conductivities ranging from 10^{-4} to 5 S/m, depending on factors such as temperature, composition, melt fraction, and melt connectivity (17–19).

Magnetic data useful for induction studies were obtained by the Galileo spacecraft from Io on four passes, labeled I24, I27, I31, and I32. The I24 and I27 passes are especially useful because they probed low Io latitudes, where the induction signature maximizes, and occurred when Io was outside of the dense part of the jovian plasma sheet near the time of maximum inducing field (>500 nT). For these near-equatorial flybys, in the Cartesian coordinate system called $I\phi\Omega$, with x parallel to Io's orbital velocity, y directed toward Jupiter, and z completing the orthogonal triad, induction contributed minimally to the B_z component, allowing us to focus on the fit to the observed B_z profile to validate our plasma interaction model and on the B_x and B_y components to establish the magnitude of the inductive response. I31 and I32 are less valuable for induction studies because they probed polar regions where the expected induction field is weak as compared with the field perturbations imposed by interaction with jovian plasma.

Near Io, field perturbations arise from both external and internal sources. Magnetohydrodynamic (MHD) perturbations result from the interaction of Io's atmosphere with Jupiter's corotating plasma (21). There, the jovian plasma is slowed by mass loading, charge exchange, and interaction with Io's conducting ionosphere.

Alfvénic perturbations called Alfvén wings couple Io to Jupiter's ionosphere, exerting forces that drive mass-loaded plasma toward corotation (22). We calculated this interaction field from a three-dimensional MHD simulation model (23) analogous to that used successfully for interpreting data acquired near Ganymede (24). An additional perturbation source is the inductive response of Io to the first three rotational harmonics (12.953, 5.619, and 4.962 hours) in Jupiter's field.

The vector amplitudes (in nanoteslas) of the three harmonics are (309, 734, 118), (70, 106, 11), and (10, 14, 1) in the $I\phi\Omega$ coordinate system. The second and third harmonics are excited by the quadrupolar and octupolar terms of Jupiter's internal dynamo. To model the inductive response to this multifrequency primary field, we used multiple-shell models of internal conductivity (25). In the models, the cold crust had zero conductivity and a thickness of 50 km (6). To obtain

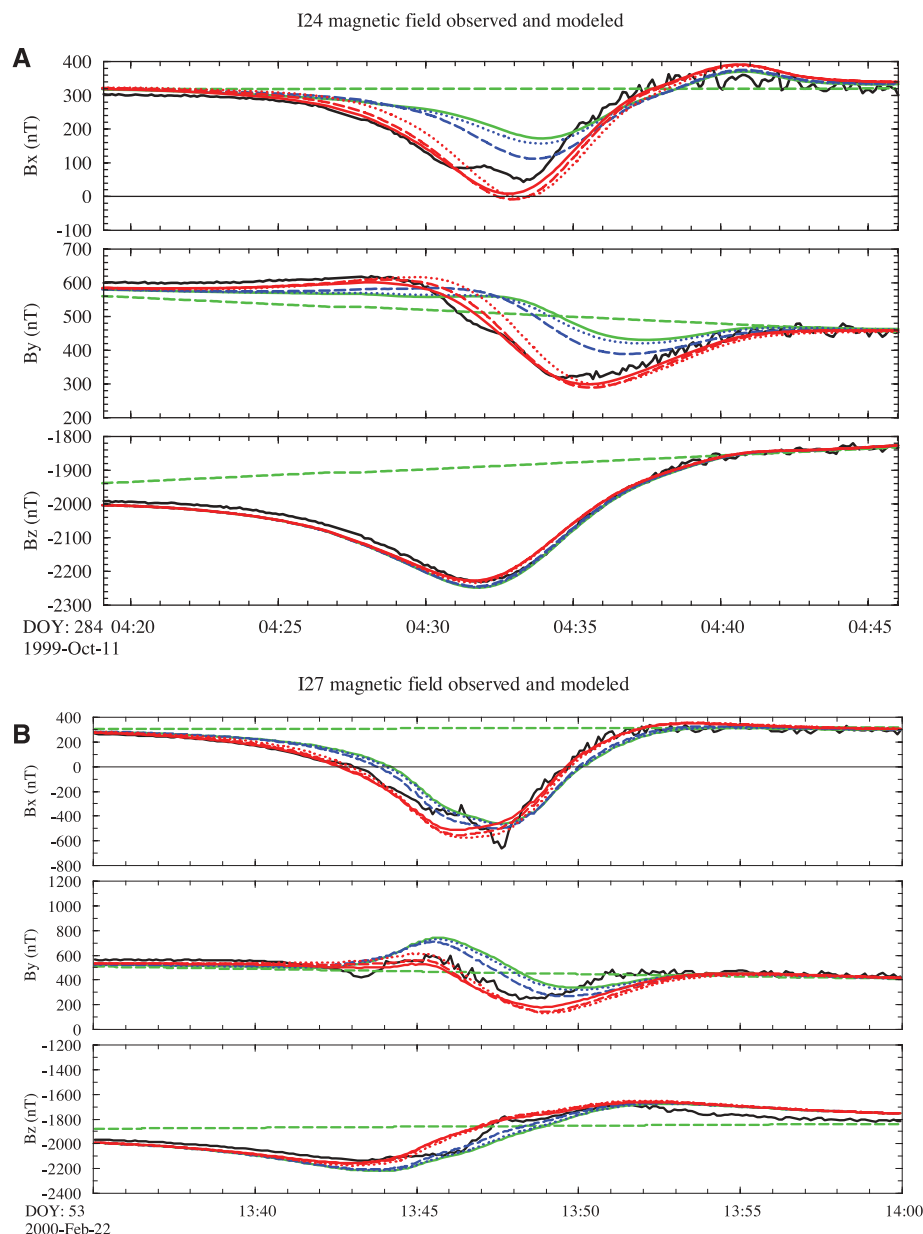


Fig. 1. (A) Observations (solid black curves) and model fields (colored lines) for the I24 pass. The dashed green line represents the jovian background field near Io. The MHD model (no induction) is plotted with solid green lines. The MHD models that include the inductive field from the following are shown: a warm solid mantle at 1200°C (conductivity = 0.002 S/m, dotted blue lines), a hot solid mantle at 1400°C (conductivity = 0.007 S/m, dashed blue lines), an asthenosphere with a 5% melt fraction (conductivity = 0.1 S/m) overlying a hot solid mantle (dotted red lines), an asthenosphere with a 20% melt fraction (conductivity = 0.43 S/m) overlying a hot solid mantle (dashed red lines), and a perfectly conducting shell located underneath the crust (solid red lines). (B) Same as (A), except for the I27 pass.

¹Institute of Geophysics and Planetary Physics, University of California at Los Angeles, Los Angeles, CA 90095, USA. ²Department of Atmospheric, Oceanic and Space Sciences, University of Michigan, Ann Arbor, MI 48109-2143, USA. ³Department of Earth and Planetary Sciences, University of California Santa Cruz, Santa Cruz, CA 95064, USA.

*To whom correspondence should be addressed. E-mail: kkhurana@igpp.ucla.edu

the conductivity of the mantle, we assumed that Io has fully differentiated (3), starting from a chondritic bulk composition (8). After the removal of silicate-rich material for a 30- to 50-km crust and of iron to form a core with a radius of 900 to 1000 km, the three main constituents remaining in the mantle were SiO₂, MgO, and FeO with weight %'s of 44, 32, and 14% (8). A good Earth analog for this type of rock is a lherzolite (derived from Spitzbergen, Norway), an ultramafic igneous rock believed to be derived from Earth's upper mantle (18). We used the electrical properties of this rock (18) to simulate Io's mantle.

As in earlier work on Europa's subsurface ocean, the solutions to the electromagnetic diffusion equation for the multiple-shell model with a perfectly conducting core were expressed in terms of Bessel functions (14, 25). The amplitude and phase responses were computed from all three jovian rotational harmonics and then summed and used to represent the internal field of Io in an MHD simulation. Even though MHD models with induction from a solid mantle fit the observations better than a model without an inductive layer, the fits were unsatisfactory (Fig. 1).

To refine the modeling further, we explored three-layer models in which a conducting asthenosphere overlies a solid mantle (Fig. 2). Even for a warm solid mantle [with conductivity (σ_1) = 0.002 S/m], the primary signal does not penetrate to the core, thus no appreciable induction is expected from the core and the conductivity of the core becomes irrelevant. Figure 2 demonstrates that for asthenospheric conductivity, $\sigma_0 \rightarrow 1$ S/m (expected in rocks with >20% melt fraction), induced fields >600 nT can be generated near Io. Further, asthenospheric thickness (h) cannot be established when it exceeds 100 km, because the response saturates. However, σ_0 and hence the melt fraction of the asthenosphere can still be inferred.

With little guidance available on asthenospheric thickness and melt fraction from tidal dissipation models (11, 26–28), we treated these as fit parameters of our model. We obtained the conductivity of the partial melt from the melt fraction using an empirical relationship derived from laboratory experiments performed on ultramafic rocks from Earth's upper mantle (17, 19). Responses from all three jovian spin harmonics were included. It is clear that an asthenospheric melt fraction $\geq 20\%$ is required for a satisfactory model of the measurements from the I24 and I27 flybys (Fig. 1). Thus, our work shows that Io currently hosts a partially or fully molten asthenosphere, with a thickness exceeding 50 km and a melt fraction of at least a few tens of percent. Current observations from Galileo are inadequate to place any stronger limits on h . Signals at longer than 13-hour periodicity are required to probe more deeply into Io's interior.

We fitted the difference fields (observations minus MHD responses without induction) from the four flybys to equatorial magnetic dipoles

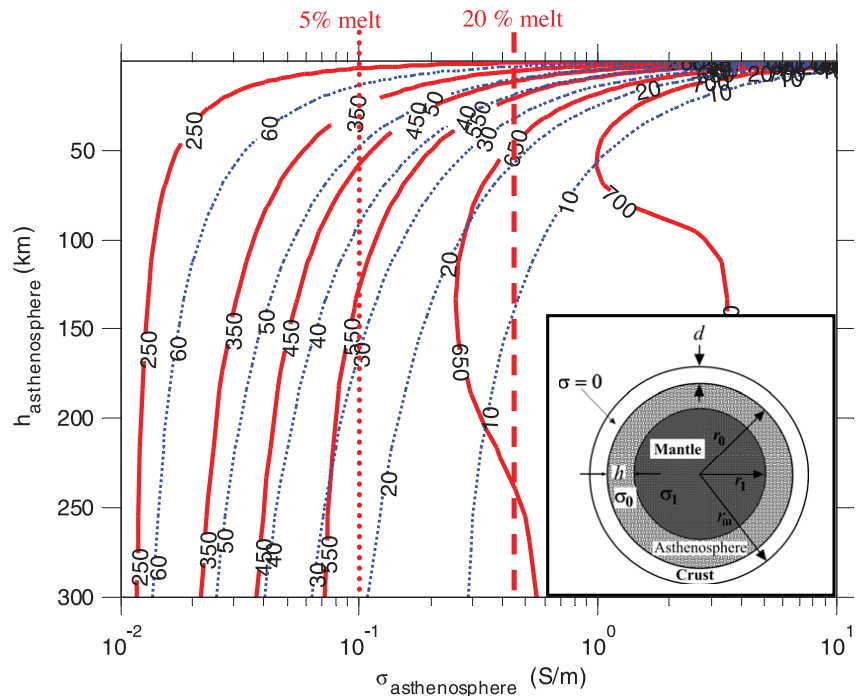


Fig. 2. The amplitude in nanoteslas at the pole of the induced dipole on Io's surface (labels on red curves) and the phase delay in degrees (labels on dotted blue curves) of the magnetic field for a three-layer model of Io consisting of a crust, a partially molten asthenosphere, and a hot solid mantle (inset) for a range of asthenospheric conductivities (x axis) and thicknesses (y axis). The period and amplitude of the inducing field were assumed to be 12.953 hours and 800 nT.

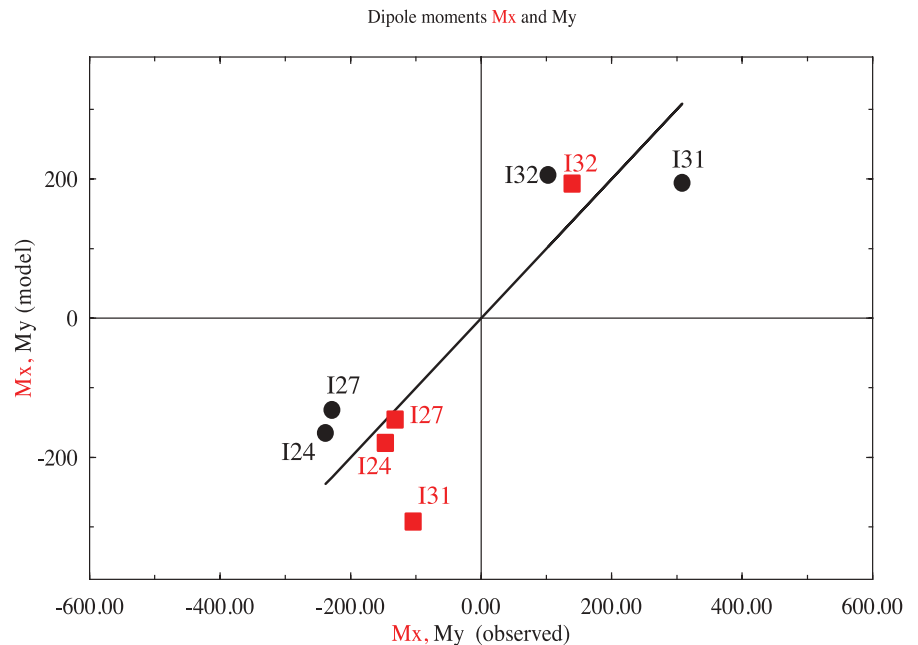


Fig. 3. The components of the observed dipole moments [ordinate, M_x (red squares) and M_y (black circles)] for the four flybys plotted against those expected from a 100% induction model (abscissa). The black solid line has a slope of unity.

(Fig. 3). Even though there is some scatter, it is clear that the observations require induction from a globally distributed good conductor. The observed dipole moment changes in strength

and direction in response to the changing primary field, ruling out a dynamo-generated field. The form of the observed field (dipolar and global) rules out localized regions of melt as

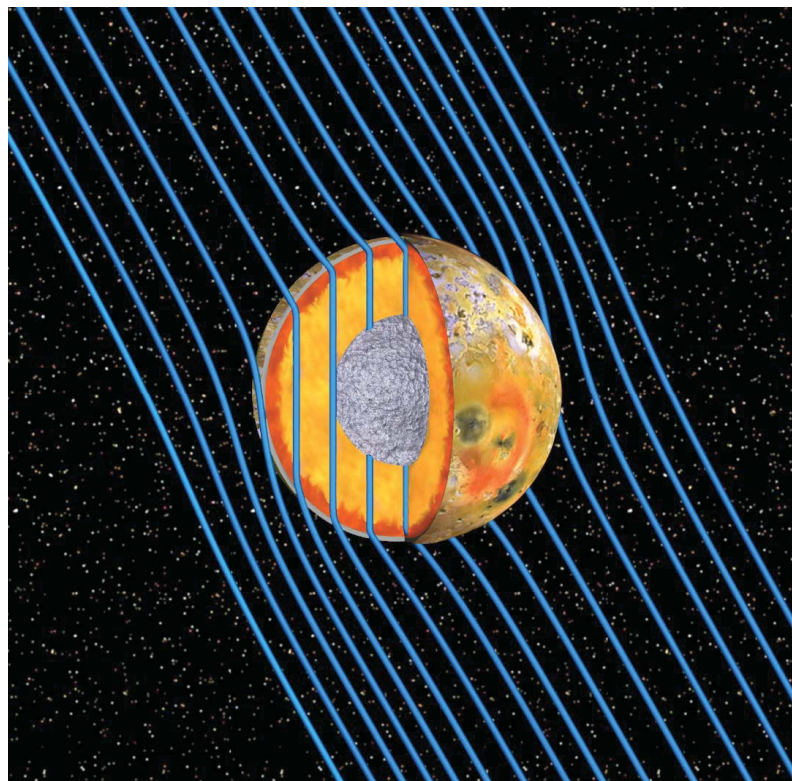


Fig. 4. The internal structure of Io as revealed by the present study. Underneath a low-density crust 30 to 50 km thick (gray outline in the cross section) exists a global magma layer (asthenosphere) with a thickness exceeding 50 km and a rock melt fraction of a few tens of percent (red-brown outline). The high electrical conductivity of the asthenosphere prevents the time-varying horizontal component of the jovian field from significantly penetrating into the mantle. The almost constant vertical magnetic field pervades the ultramafic mantle (golden hues in cross section), which must have a temperature exceeding 1200°C to support rock melts in the asthenosphere. The 600- to 900-km-radius core composed of Fe-FeS is rendered in a metallic silver hue.

sources, because such unconnected conductors would induce higher-order spherical harmonics (which we did not observe), with a dipolar moment much weaker than the saturated response that we observed. On the other hand, a global layer of interconnected melts is a valid explanation for our data.

After subtracting the MHD + inductive response (calculated from our 20% melt model) from the observations, we inverted the residual fields from the four flybys for a common dipole moment. The value (−38.2, 73.6, 67.5) nT obtained for the dipole moment in $I\phi\Omega$ coordinates shows that if Io has a permanent internal magnetic field, it is extremely weak.

The presence of a partially molten asthenosphere (Fig. 4) in Io supports the idea that Io's mantle is too hot to effectively cool its core, thus explaining the apparent absence of a dynamo (29) and making it more likely that Io's core is completely molten. This result marks the asthenosphere as a primary site of tidal heating and allows us to predict that Io's heat flux, if predominantly due to tidal heating in the asthenosphere, will be higher in equatorial regions as compared to the poles (26). Lateral variations of asthenospheric

thickness and/or melt fraction that would arise from non-uniform heating modify the magnetic induction spectrum at frequencies not resolved in our data set.

References and Notes

- G. J. Veeder, D. Matson, T. Johnson, D. Blaney, J. Gougen, *J. Geophys. Res.* **99**, 17095 (1994).
- J. A. Rathbun *et al.*, *Icarus* **169**, 127 (2004).
- J. D. Anderson, R. A. Jacobson, E. L. Lau, W. B. Moore, G. S. Schubert, *J. Geophys. Res.* **106**, 32,963 (2001).
- W. B. Moore, G. Schubert, J. D. Anderson, J. S. Spencer, in *Io After Galileo*, R. M. C. Lopes, J. R. Spencer, Eds. (Springer-Praxis, Chichester, UK, 2007), pp. 89–108.
- F. Sohl, D. Spohn, D. Breuer, K. Nagel, *Icarus* **157**, 104 (2002).
- L. Keszthelyi, A. McEwen, *Icarus* **130**, 437 (1997).
- L. Keszthelyi, A. S. McEwen, G. J. Taylor, *Icarus* **141**, 415 (1999).
- L. Keszthelyi *et al.*, *Icarus* **192**, 491 (2007).
- M. N. Ross, G. Schubert, *Icarus* **64**, 391 (1985).
- J. R. Spencer, N. M. Schneider, *Annu. Rev. Earth Planet. Sci.* **24**, 125 (1996).
- M. Segatz, T. Spohn, M. N. Ross, G. Schubert, *Icarus* **75**, 187 (1988).
- L. Keszthelyi, W. L. Jaeger, E. P. Turtle, M. Milazzo, J. Radebaugh, *Icarus* **169**, 271 (2004).
- K. K. Khurana *et al.*, *Nature* **395**, 777 (1998).
- C. Zimmer, K. K. Khurana, M. G. Kivelson, *Icarus* **147**, 329 (2000).

- M. G. Kivelson, K. K. Khurana, M. Volwerk, *Icarus* **157**, 507 (2002).
- M. C. Sinha *et al.*, *Philos. Trans. R. Soc. London Ser. A* **355**, 233 (1997).
- G. M. Partzsch, F. R. Schilling, J. Arndt, *Tectonophysics* **317**, 189 (2000).
- J. Maumus, N. Bagdassarov, H. Schmeling, *Geochim. Cosmochim. Acta* **69**, 4703 (2005).
- F. R. Schilling, G. M. Partzsch, H. Brasse, G. Schwarz, *Phys. Earth Planet. Inter.* **103**, 17 (1997).
- G. R. Olhoeft, in *Physical Properties of Rocks and Minerals*, Y. S. Touloukian, W. R. Judd, R. F. Roy, Eds. (Hemisphere Publishing, New York, 1989), pp. 257–329.
- An earlier simulation of I24 and I27 flybys (30) treated the multifluid nature of the atmosphere and the plasma with sophistication but sacrificed self-consistency of the magnetic field. Furthermore, the large perturbations obtained in that simulation were found in a run using upstream plasma conditions that were markedly different from those measured on the passes we analyzed.
- F. M. Neubauer, *J. Geophys. Res.* **103**, 19843 (1998).
- X. Jia, R. J. Walker, M. G. Kivelson, K. K. Khurana, J. A. Linker, *J. Geophys. Res.* **114**, A09209 (2009).
- Materials and methods are available as supporting material on Science Online.
- W. D. Parkinson, *Introduction to Geomagnetism* (Scottish Academic Press, Edinburgh, 1983).
- M. N. Ross, G. Schubert, T. Spohn, R. W. Gaskell, *Icarus* **85**, 309 (1990).
- H. Fischer, J. T. Spohn, *Icarus* **83**, 39 (1990).
- W. B. Moore, *Icarus* **154**, 548 (2001).
- U. Weinbruch, T. Spohn, *Planet. Space Sci.* **43**, 1045 (1995).
- J. Saur, F. M. Neubauer, D. F. Strobel, M. E. Summers, *J. Geophys. Res.* **107**, 1422 (2002).
- E. Lellouch, *Space Sci. Rev.* **116**, 211 (2005).
- J. R. Spencer *et al.*, *Icarus* **176**, 283 (2005).
- L. M. Feaga, M. McGrath, P. D. Feldman, *Icarus* **201**, 570 (2009).
- R. E. Johnson, *Astrophys. J.* **609**, L99 (2004).
- M. C. Wong, W. H. Smyth, *Icarus* **146**, 60 (2000).
- R. E. Johnson *et al.*, in *Jupiter: The Planets, Satellites and Magnetosphere*, F. Bagenal, T. E. Dowling, W. B. McKinnon, Eds. (Cambridge Univ. Press, Cambridge, 2004), pp. 485–512.
- J. A. Linker, K. K. Khurana, M. G. Kivelson, R. J. Walker, *J. Geophys. Res.* **103**, 19,867 (1998).
- X. Jia, R. J. Walker, M. G. Kivelson, K. K. Khurana, J. A. Linker, *J. Geophys. Res.* **113**, A06212 (2008).
- M. A. McGrath, R. E. Johnson, *J. Geophys. Res.* **94**, (A3), 2677 (1989).
- L. A. Frank, W. R. Paterson, *J. Geophys. Res.* **105**, 25,363 (2000).
- L. A. Frank, W. R. Paterson, *J. Geophys. Res.* **106**, 26,209 (2001).
- L. A. Frank, W. R. Paterson, *J. Geophys. Res.* **107**, 1220 (2002).
- D. A. Gurnett, A. M. Persoon, W. S. Kurth, A. Roux, S. J. Bolton, *J. Geophys. Res.* **106**, 26,225 (2001).

Acknowledgments: The work at the University of California at Los Angeles was supported by NASA grant NNX08AT48G and NSF Planetary Astronomy grant AST-0909206. The field and plasma data used in this work are available online on the Planetary Data System at <http://ppi.pds.nasa.gov/search/?s=GALILEO%20ORBITER>.

Supporting Online Material

www.sciencemag.org/cgi/content/full/science.1201425/DC1
SOM Text
References (31–43)

8 December 2010; accepted 15 April 2011
Published online 12 May 2011;
10.1126/science.1201425